engineering proceedings

MDPI

Proceeding Paper

Cluttered Environment and Target Simulator to Evaluate Primary Surveillance Radar Processors †

Fernando Lara [1,*], Ricardo Mena [1], Antonio Flores [1], Felipe Grijalva [2] and Roman Lara-Cueva [3,4]

[1] Departamentro de Electrónica, Telecomunicaciones y Redes de Información (DETRI), Escuela Politécnica Nacional, Quito 170525, Ecuador; ricardo.menav@epn.edu.ec (R.M.); luis.flores04@epn.edu.ec (A.F.)
[2] Colegio de Ciencias e Ingenierías "El Politécnico", Universidad San Francisco de Quito USFQ, Quito 170157, Ecuador; fgrijalva@usfq.edu.ec
[3] Grupo de Investigación en Sistemas Inteligentes (WiCOM-Energy), Departamento de Ingeniería Eléctrica, Electrónica y Telecomunicaciones, Universidad de las Fuerzas Armadas ESPE, Sangolquí 171103, Ecuador; ralara@espe.edu.ec
[4] Ad Hoc Networks Research Center (CIRAD), Departamento de Ingeniería Eléctrica, Electrónica y Telecomunicaciones, Universidad de las Fuerzas Armadas ESPE, Sangolquí 171103, Ecuador
* Correspondence: marco.lara@epn.edu.ec
† Presented at the XXXI Conference on Electrical and Electronic Engineering, Quito, Ecuador, 29 November–1 December 2023.

Abstract: This research article presents a comprehensive study focusing on advancing radar systems for unmanned aerial vehicle (UAV) surveillance in cluttered environments. The proliferation of UAV technology and its diverse applications have raised concerns about airspace security. To tackle this issue, this article introduces a novel simulator designed to evaluate the performance of primary monopulse radar processors. The simulator accurately replicates scenarios involving clutter Weibull distributions, stationary and moving targets, as well as pulse compression situations, thereby enabling precise and controlled evaluations. The study employs the simulator to assess radar processors, including a variant of moving target detection (MTD) and a constant false alarm rate (CFAR) processor. By implementing a rigorous methodology, the article underscores the significance of simulating cluttered conditions in refining the effectiveness of radar processors. The results yield valuable insights, facilitating objective interpretations. The proposed simulator and its implications contribute to enhancing UAV surveillance and airspace security, thereby pushing forward the capabilities of radar systems.

Keywords: cluttered environments; radar simulator; MTD and CFAR processors

check for updates

Citation: Lara, F.; Mena, R.; Flores, A.; Grijalva, F.; Lara-Cueva, R. Cluttered Environment and Target Simulator to Evaluate Primary Surveillance Radar Processors. *Eng. Proc.* **2023**, *47*, 14. https://doi.org/10.3390/engproc2023047014

Academic Editor: Fernando Carrera Suarez

Published: 4 December 2023

Copyright: © 2023 by the authors. Licensee MDPI, Basel, Switzerland. This article is an open access article distributed under the terms and conditions of the Creative Commons Attribution (CC BY) license (https://creativecommons.org/licenses/by/4.0/).

1. Introduction

The new technological advancements in UAVs and the increasing number of civil or non-military applications [1] threaten the security of the airspace [2]. This underscores the imperative need to enhance the capabilities of surveillance and object detection systems. Radar systems (radio detection and ranging), known for their robust performance in complex environments by accurately determining the azimuthal position, distance, and velocity of UAVs, as discussed in [3], assume a pivotal role. Furthermore, their real-time responsiveness makes these systems a fundamental tool for governmental entities when making decisions regarding UAV intrusion into restricted aerial spaces.

UAVs are known to have a limited radar cross-section (RCS), which is a measure of how detectable an object is by radar systems [4]. Objects with a smaller RCS are harder to detect with radar because they reflect less radar energy back to the receiver. UAVs are designed to have a small RCS to minimize their radar signature and make them less visible to radar systems. Therefore, it is necessary to develop new processors capable of detecting targets in environments with a signal to clutter ratio (SCR) close to 0. Traditional

processors like the moving target indicator (MTI) described in [5] and the moving target detection (MTD) discussed in [6] are presently employed in primary surveillance systems, as referenced in [7–9]. For the detection of UAVs in urban settings, novel processors based on artificial intelligence, as mentioned in [10], and multiple-input–multiple-output (MIMO) systems, discussed in [11,12], among other approaches, are being tested.

To enhance and assess the performance of the processors, controlled environments are essential. Furthermore, training machine learning and deep learning systems requires substantial volumes of data, which, due to operational costs, prove challenging to acquire.

Hence, various simulated environments have been proposed. In [13], the simulation of cloud position acquisition through radar systems is presented, aimed at training prediction systems. In [14], a 77 GHz radar simulator for adaptive cruise control is introduced, where the complete frequency modulated continuous wave (FMCW) radar platform is simulated and different algorithm enhancements are tested. In [15], a radar simulator for human activity is presented, considering micro-Doppler effects. Finally, in [16], a maritime environment simulator for primary radars is showcased. This simulator incorporates empirical sea clutter parameters into a model used to simulate a maritime setting. In [17], a radar signal generation tool based on weather time series is presented to test radar processors. In [18], the use of a radar for the recognition of human activities is presented; synthetic data are generated from initial spectrograms with image transformation.

The accurate simulation of cluttered environments offers significant advantages in terms of economic savings, time efficiency, and effectiveness. This enables the evaluation of radar processor performance and the adjustment of key parameters before the physical implementation of those processors. To the best of our knowledge, no simulators have been found for primary monopulse radars in environments with ground clutter.

This article proposes the configuration of a clutter and target simulator to assess primary monopulse surveillance radar processors. The proposed system simulates Weibull clutter, stationary targets, and moving targets with or without pulse compression (Swerling 0) [19]. The generated simulator is tested with two radar processors, a variant of moving target detection (MTD) [20] and a constant false alarm rate (CFAR) processor [21], in order to develop a tool that permits the assessment and testing of radar design before its implementation.

Section 2 outlines the implementation methodology and the tests conducted on the simulator. In Section 3, the results and discussion are presented. Finally, Section 4 offers conclusions and outlines future work.

2. Materials and Methods

The objective of this article is to generate two matrices that simulate the signals acquired by monopulse surveillance radars. These arrays contain simulated in-phase (I) and quadrature (Q) signals, considering Gaussian noise, ground clutter, and targets. The implementation of the radar signal simulator is described in Section 2.1. The tests conducted with the simulated I/Q signals are presented in Section 2.2.

2.1. Simulator

2.1.1. Clutter model

The Weibull clutter model is represented by Equation (1):

$$c[n] = w_c[n] + \alpha c[n-1], \tag{1}$$

where $c[n]$ represents the clutter signal obtained, $w_c[n]$ corresponds to additive Gaussian noise, and α is the correlation coefficient, which depends on the radar's integration pulses. For short-range surveillance radars (with high antenna rotation speeds), it is recommended to have $\alpha > 0.8$, while for long-range surveillance radars, $\alpha < 0.8$ is advised.

In Figure 1, an example of a generated clutter signal is depicted. This clutter corresponds to ground reflections of the generated signal.

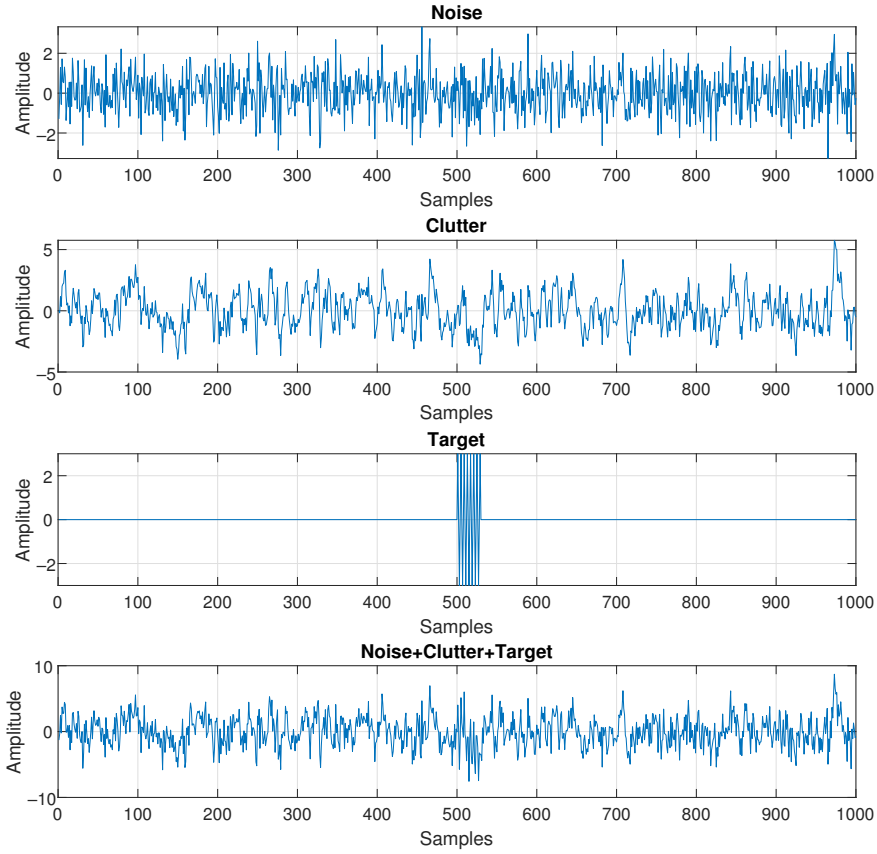

Figure 1. Simulated radar ring (Gaussian noise, clutter, and target).

2.1.2. Target Model

The number of pulses to be integrated (pulses that illuminate a target in a resolution cell) is defined by Equation (2).

$$N = \frac{\phi}{6\omega T} = \frac{\phi \times PRF}{6\omega}, \tag{2}$$

where N is the number of pulses to be integrated, ϕ is the beamwidth of the radar antenna's main lobe (measured at the half-power points of the beam), ω is the antenna rotation speed in RPM (revolutions per minute), and T is the pulse repetition period, which can be expressed as $PRF = \frac{1}{T}$ (pulse repetition frequency).

With these parameters, a number of samples can be determined for simulating the target. The target model used is presented in Equation (3), which corresponds to a target with Doppler shift and Swerling 0 characteristics [3,19].

$$s[n] = A \sin(2\pi f_d n), \tag{3}$$

where A is the amplitude of the target and f_d is the Doppler frequency. An example of a target signal is shown in Figure 1.

The simulator includes a module for simulating expanded pulses with bi-phase codes, such as Barker codes [22]. To achieve this, the code vector needs to be provided. For instance, $b[n]$ is a Barker code of length 5: $b[n] = [+1, +1, +1, -1, +1]$. To obtain the expanded pulse, Equation (4) is used.

$$S_E[n] = [s_1[n]b[2], s_2[n]b[2], \ldots, s_M[n]b[M]], \tag{4}$$

where M represents the pulse length.

2.1.3. Integration of the System

The radar target detection problem can be formulated as a binary hypothesis, as shown in Equation (5). The null hypothesis represents the absence of a target and includes the addition of noise $w[n]$ and clutter $c[n]$. The alternative hypothesis includes the target $s[n]$ in addition to noise and clutter.

$$\begin{aligned} H_0 &: r[n] = w[n] + c[n], n = 0, 1, 2, 3, ..., N \\ H_1 &: r[n] = w[n] + c[n] + s[n], n = 0, 1, 2, 3, ..., N. \end{aligned} \tag{5}$$

This concept from Equation (5) is used to generate the simulated I/Q signals, where noise, clutter, and/or target signals can be added to each cell (see Figure 1). The aggregation of cells generates a radar ring, which is integrated as shown in Figure 2.

In addition, Figure 2 demonstrates an example of ring integration, illustrating correlated clutter within cells of the same ring and no correlation between rings. This background noise is complemented by cells with target signals. The number of integration pulses depends on the physical characteristics of the radar, as discussed in the previous section.

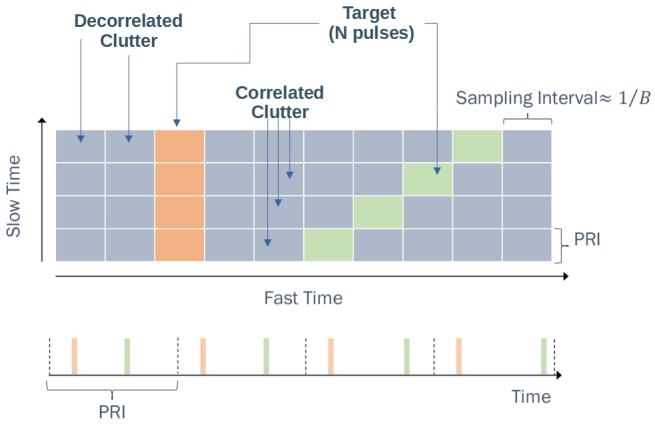

Figure 2. Data matrix integration.

The number of rings is related to the resolution cells, radar range (Equation (6)), the cone of silence, and the sampling frequency. The number of samples per ring depends on the PRF.

$$R_d = \frac{c \times \delta}{2}, \tag{6}$$

where R_d is the length of the cell, c is the speed of light, and δ is the pulse duration. In the case of coded pulses, δ represents the pulse duration relative to the code length.

Controlling the signal-to-clutter ratio (SCR) is an advantage of using a simulated environment, considering Equation (7).

$$SCR = \frac{P_{target}}{P_{noise} + P_{clutter}} = \frac{P_S}{P_W + P_C}, \tag{7}$$

where P_S is the power of the signal reflected from the target, P_W is the power of the noise signal, and P_C is the power of the clutter signal.

The generated test environments correspond to a Skyguard Oerlikon radar [20] (surveillance radar with a range of 16 km) and an AN/TPS 70 radar [23] (surveillance radar with a range of 440 km). These environments are used to evaluate the MTD and CFAR processors.

2.2. Testing

Firstly, the simulated signals undergo a high-pass filter designed to accentuate high-frequency components and focus on relevant target characteristics, thereby enhancing the quality of the observed signals. Subsequently, a decompression process is implemented using known codes, enabling the recovery of efficiently encoded target information for transmission or storage. By reconstructing the original signal, subsequent processing and analysis are facilitated. Following this, a magnitude detector is introduced, identifying significant peaks in the processed signals, a pivotal step for accurate target detection in the presence of clutter. Additionally, the constant false alarm rate (CFAR) algorithm is implemented, automatically adjusting the detection threshold based on local noise levels while maintaining a constant false alarm rate, further enhancing the detection system's reliability.

Lastly, the persistent challenge of stationary clutter in cluttered environments is tackled via a suppression algorithm rooted in target detection. This implementation significantly contributes to the reduction in false alarms and, importantly, optimizes precision in identifying moving targets.

Processors

In order to verify the environment generation, two traditional radar processors are employed, the MTD processor, for monopulse targets without pulse compression [6,20,24] (as shown in Figure 3a), and the CFAR processor, for pulse-compressed targets [19,21], using Barker code [22,25] (as depicted in Figure 3b).

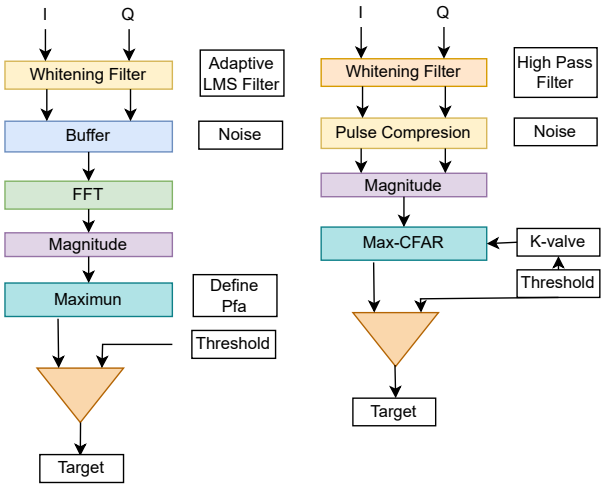

(**a**) (**b**)

Figure 3. Radar processors. (**a**) MTD. (**b**) CFAR.

These processors generate a detection vector with information on azimuth, distance, and whether the target is stationary or mobile. This information is displayed on a plan position indicator (PPI) display.

3. Results and Discussion

To evaluate the controlled SCR simulated environment, two recordings are generated: one simulating acquisition parameters for an AN/TPS 70 radar and the second simulating acquisition with an Oerlikon Skyguard radar. The respective processors are then applied. For the AN/TPS 70 case, a Barker code pulse compression magnitude detector CFAR is used, while for the Oerlikon Skyguard case, an MTD processor is employed.

3.1. AN/TPS 70

In Figure 4, the phase of the simulated 10 s record (one rotation) is presented, considering a PRF of 250 Hz and a sampling frequency in mega samples per second equal to 4. The entire environment is assumed to exhibit reflections with a correlation coefficient of 0.6, in addition to three regions of elevated ground clutter magnitude. The environment contains six targets (see Table 1), which were simulated with different integration numbers, equivalent to simulating targets of varying sizes. All simulated targets have an SCR of 3 dB and three concentrations of ground clutter (azimuth: $0.012\pi, 1.92\pi, 0.92\pi$; and range: 27.5 km, 192.5 km, 421.7 km) within a 3 km dimension.

Table 1. Simulated targets for AN/TPS 70.

Target Number	Range (km)	Azimuth (rad)	Integration Pulse
1	37.4	0.0π	8
2	11.7	1.9π	12
3	184.1	1.0π	7
4	274.3	0.6π	5
5	367.4	0.1π	10
6	402.6	1.6π	9

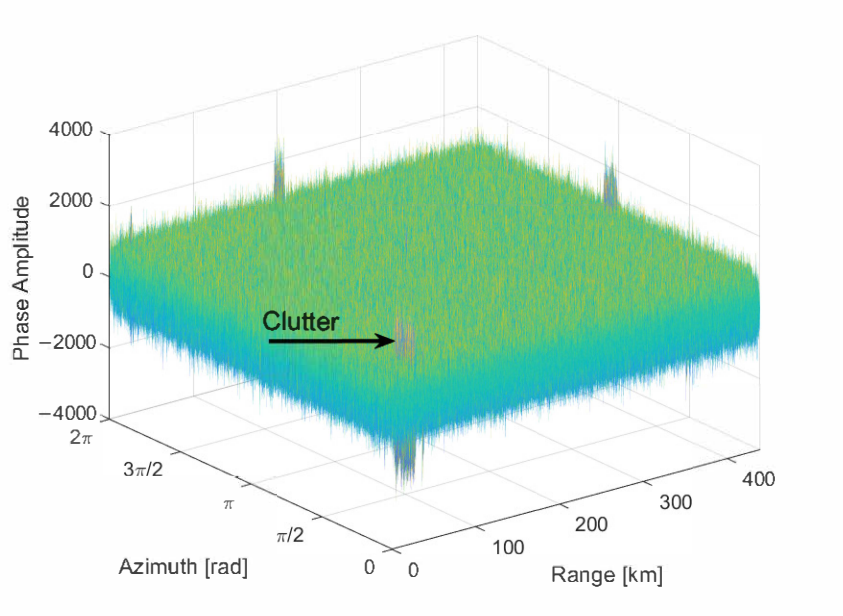

Figure 4. Simulated environment with targets and clutter (AN/TPS 70).

In Figure 5a, the output of a high-pass filter (clutter whitening filter) is presented. As observed in the figure, clutter is attenuated, though the targets are not yet discernible. The simulator's purpose is to test the capabilities of each stage of a radar processor.

The next stage involves a compression process using a Barker code. In Figure 5b, peaks with magnitudes higher than the noise level can be observed. These peaks are associated with the targets. The presented information only represents the phase. Combining the phase and quadrature information, the magnitude is obtained (see Figure 5c).

To distinguish targets from noise, a max CFAR processor [21] is applied. The output of this processor is shown in Figure 5d.

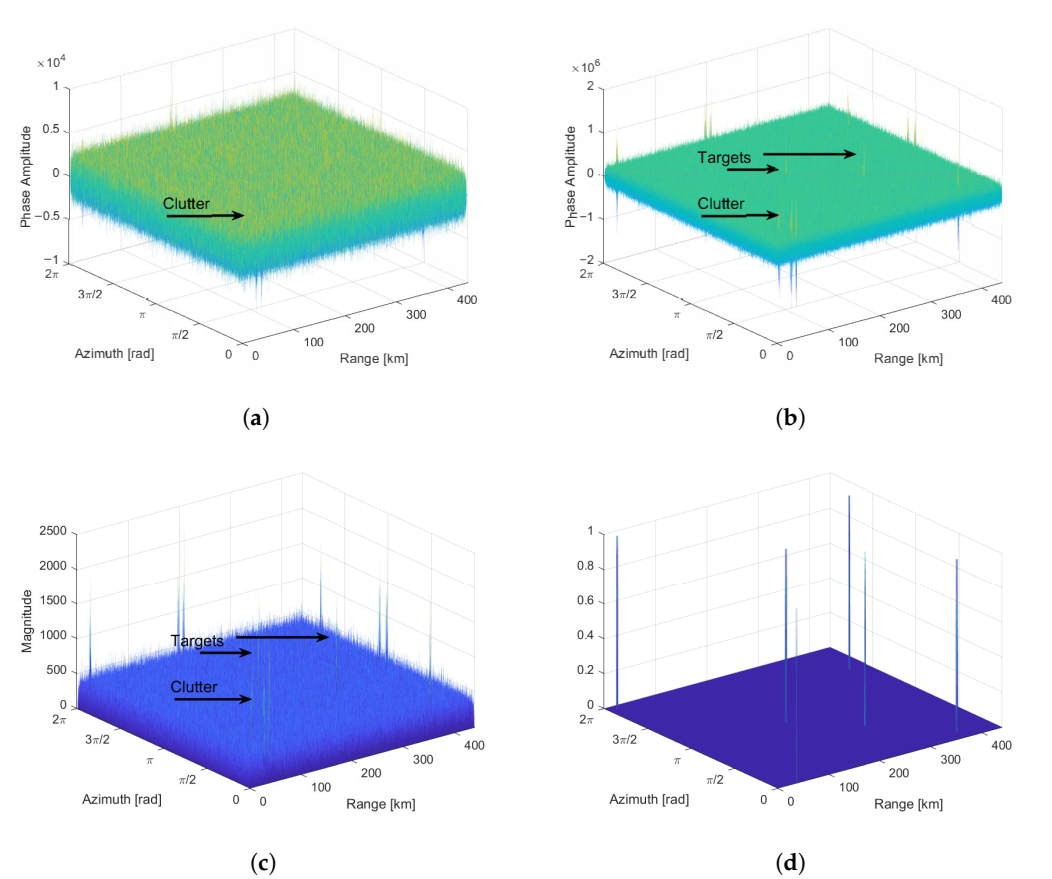

(**a**) (**b**)

(**c**) (**d**)

Figure 5. Target detection. (**a**) Simulated environment passed through a clutter whitening filter. (**b**) Environment passed by pulse compression. (**c**) Magnitude of simulated environment. (**d**) Target detection with threshold.

As a final stage, stationary clutter is removed by utilizing the simulator's capability to generate moving targets. This allows for varying the target's position during each rotation (10 s). In this case, information from four rotations (120,000,000 complex I/Q data points) is used. If a target remains in the same position for at least three rotations, it is considered a stationary target. Otherwise, it is considered a moving target and displayed on the PPI display, as seen in Figure 6.

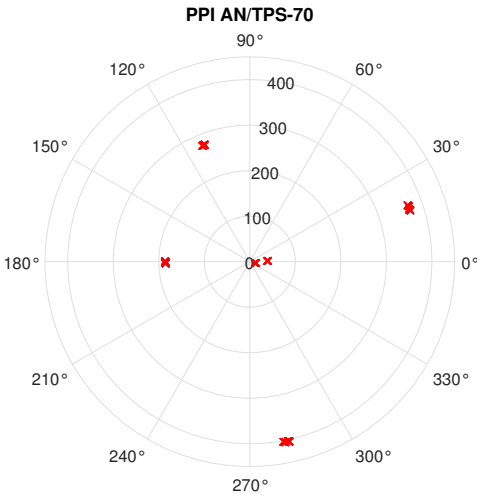

Figure 6. PPI simulation of AN/TPS 70.

3.2. Oerlikon Skyguard

A real application of the applicability of these simulators is in the Oerlikon Skyguard air defense system. The developed simulator generates various matrices with noise, clutter, and targets. Additionally, it associates target information and presents it on a PPI display. Targets can be labeled as either stationary or mobile based on their presentation on the PPI.

In the case of simulating phase and quadrature signals from Oerlikon Skyguard, a PRF of 6900 Hz is considered, a sampling frequency of 5 mega samples per second is considered, with a rotation speed of 1 RPM. With these data for the Oerlikon Skyguard radar, 5,000,000 complex I/Q data points are simulated per second. The targets on the Oerlikon Skyguard radar do not have pulse compression; considering Equation (2) with the characteristics of Oerlikon Skyguard there are 33 integration pulses and 150 m cells per simulated objective.

Figure 7a presents the radar environment for the Oerlikon Skyguard system. It displays radar returns over time or azimuth, with prominent peaks indicating detected targets, such as aircraft, and smaller, scattered returns representing clutter from the surrounding environment. The graph provides insights into the radar's ability to distinguish between targets and clutter.

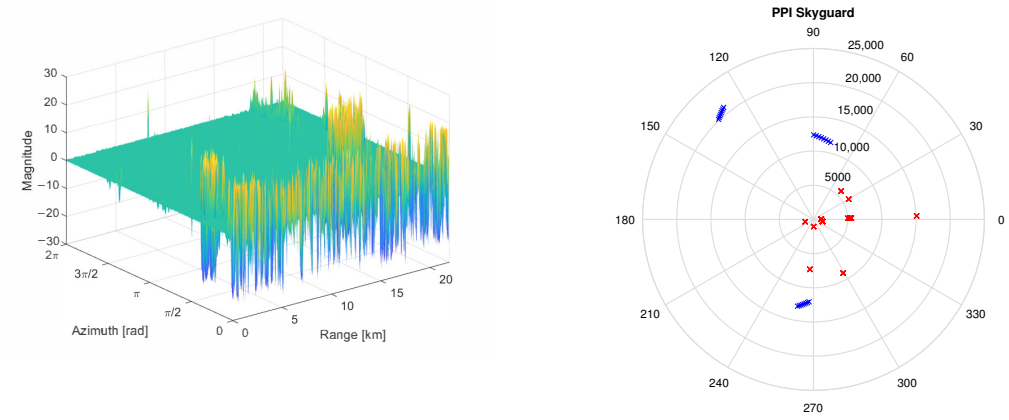

(**a**) (**b**)

Figure 7. Environment for Oerlikon Skyguard. (**a**) Environment with clutter and targets; (**b**) PPI.

In Figure 7b, the Oerlikon Skyguard radar's coverage area is presented in the PPI diagram. It centers around the radar's location, with concentric circles representing distance. Detected targets are symbolized on the display, showing their positions in relation to the radar's azimuth and range.

The original Oerlikon Skyguard system has an MTI processor, with a detection probability of 80%, with an SCR of 9 dB, and a false alarm probability of 10^{-5} [20,24]. By using simulated environments to train processors with machine learning and deep learning, the theoretical capabilities are increased, with a detection probability of 90%, an SCR from -3 dB to 0 dB, and a false alarm probability of 10^{-5} [10]. With these improvements in processing it is possible to detect targets with lower RCS, such as UAVs, with traditional radar systems.

4. Conclusions

The developed simulator presents a controlled platform that facilitates the evaluation of primary monopulse radar processors, enabling precise predictions of their real-world performance. By utilizing this simulator to assess various radar processor variants, such as MTD and CFAR, the study underscores the pivotal role of simulation in advancing radar technology for practical applications.

The research highlights the importance of incorporating fundamental physical radar parameters, including PRF, frequency, and range. These parameters are meticulously in-

tegrated to simulate the acquired phase and quadrature data corresponding to single or multiple radar rotations. This approach ensures the simulator's accurate replication of real-world conditions, providing an authentic assessment of primary monopulse radar processors for UAV surveillance. By incorporating these radar parameters into the simulation, the study enhances evaluation reliability and advances radar technology for practical applications, encompassing enhanced UAV surveillance and elevated airspace security.

A significant contribution of this study is the integration of controlled objectives within the context of SCR. These objectives encompass both mobile and fixed entities. By incorporating controlled objectives into the simulation, the study conducted a comprehensive evaluation of primary monopulse radar processors. This integration facilitates a meticulous assessment of how radar systems interact with dynamic and stationary targets, further refining the simulator's capability to emulate real-world scenarios. Consequently, the research offers a pragmatic avenue for refining radar technologies, their practical application, and the subsequent enhancement in UAV surveillance capabilities. This integration underscores the importance of an inclusive evaluation approach that encompasses diverse objectives and contributes to the ongoing innovation of radar system design and evaluation practices.

In the future, it is planned to improve the target model with different Swerlings, as well as different clutter models for sea clutter, among others. Additionally, it is intended to train processors based on machine learning to improve the detection capacity of current systems.

Author Contributions: Conceptualization, F.L.; methodology, F.L., F.G. and R.L.-C.; formal analysis, F.L.; investigation, F.L., F.G. and R.L.-C.; resources, F.L., F.G. and R.L.-C.; data curation, F.L. and R.M.; writing—original draft, F.L., R.M. and A.F.; writing— review and editing, F.L., R.M. and A.F.; visualization, R.M. and A.F.; supervision, F.G. and R.L.-C.; project administration, F.L. and R.L.-C.; funding acquisition, F.L. All authors have read and agreed to the published version of the manuscript.

Funding: This research received no external funding.

Institutional Review Board Statement: Not applicable.

Informed Consent Statement: Not applicable.

Data Availability Statement: No new data were created or analyzed in this study. Data sharing is not aplicable to this article.

Conflicts of Interest: The authors declare no conflict of interest.

References

1. Wellig, P.; Speirs, P.; Schuepbach, C.; Oechslin, R.; Renker, M.; Boeniger, U.; Pratisto, H. Radar systems and challenges for C-UAV. In Proceedings of the 2018 19th International Radar Symposium (IRS), Bonn, Germany, 20–22 June 2018; IEEE: Piscataway Township, NJ, USA, 2018; pp. 1–8.
2. Peacock, M.; Johnstone, M.N. Towards Detection and Control of Civilian Unmanned Aerial Vehicles. In Proceedings of the 14th Australian Information Warfare Conference, Perth, Australia, 2–4 December 2013; Edith Cowan University Security Research Institute: Perth, Australia; pp. 9–15.
3. Skolnik, M.I. *Radar Handbook*; McGraw-Hill: New York, NY, USA, 1970.
4. Farlik, J.; Kratky, M.; Casar, J.; Stary, V. Radar cross section and detection of small unmanned aerial vehicles. In Proceedings of the 2016 17th International Conference on Mechatronics-Mechatronika (ME), Prague, Czech Republic, 7–9 December 2016; pp. 1–7.
5. Tomita, Y.; Irabu, T.; Kiuchi, E. Moving Target Indication Radar. US Patent 4,053,885, 28 December 1977.
6. O'Donnell, R.; Muehe, C.; Labitt, M.; Drury, W.; Cartledge, L. Advanced signal processing for airport surveillance radars. In *IEEE Electronic and Aerospace Systems Convention (EASCON'74)*; IEEE: Piscataway Township, NJ, USA, 1974; p. 71.
7. Hyun, E.; Jin, Y.S.; Ju, Y.; Lee, J.H. Development of short-range ground surveillance radar for moving target detection. In Proceedings of the 2015 IEEE 5th Asia-Pacific Conference on Synthetic Aperture Radar (APSAR), Singapore, 1–4 September 2015; IEEE: Piscataway Township, NJ, USA, 2015; pp. 692–695.
8. Santi, F.; Pastina, D.; Bucciarelli, M. Maritime moving target detection technique for passive bistatic radar with GNSS transmitters. In Proceedings of the 2017 18th International Radar Symposium (IRS), Prague, Czech Republic, 28–30 June 2017; IEEE: Piscataway Township, NJ, USA, 2017; pp. 1–10.
9. Nag, S.; Barnes, M. A moving target detection filter for an ultra-wideband radar. In Proceedings of the 2003 IEEE Radar Conference (Cat. No. 03CH37474), Huntsville, AL, USA, 8 May 2003; IEEE: Piscataway Township, NJ, USA, 2003; pp. 147–153.

10. Carrera, E.V.; Lara, F.; Ortiz, M.; Tinoco, A.; León, R. Target detection using radar processors based on machine learning. In Proceedings of the 2020 IEEE ANDESCON, Quito, Ecuador, 13–16 October 2020; IEEE: Piscataway Township, NJ, USA, 2020; pp. 1–5.
11. Yuan, Y.; Yi, W.; Hoseinnezhad, R.; Varshney, P.K. Robust power allocation for resource-aware multi-target tracking with colocated MIMO radars. *IEEE Trans. Signal Process.* **2020**, *69*, 443–458. [CrossRef]
12. Shi, Z.; Wang, H.; Leung, C.S.; So, H.C.; Eurasip, M. Robust MIMO radar target localization based on lagrange programming neural network. *Signal Process.* **2020**, *174*, 107574. [CrossRef]
13. Haynes, J.M.; Marchand, R.T.; Luo, Z.; Bodas-Salcedo, A.; Stephens, G.L. A multipurpose radar simulation package: QuickBeam. *Bull. Am. Meteorol. Soc.* **2007**, *88*, 1723–1728. [CrossRef]
14. Kärnfelt, C.; Péden, A.; Bazzi, A.; Shhadé, G.E.H.; Abbas, M.; Chonavel, T. 77 GHz ACC radar simulation platform. In Proceedings of the 2009 9th International Conference on Intelligent Transport Systems Telecommunications, (ITST), Lille, France, 20–22 October 2009; IEEE: Piscataway Township, NJ, USA, 2009, pp. 209–214.
15. Vishwakarma, S.; Li, W.; Tang, C.; Woodbridge, K.; Adve, R.; Chetty, K. SimHumalator: An open-source end-to-end radar simulator for human activity recognition. *IEEE Aerosp. Electron. Syst. Mag.* **2021**, *37*, 6–22. [CrossRef]
16. Rosenberg, L.; Watts, S.; Bocquet, S. Scanning radar simulation in the maritime environment. In Proceedings of the 2020 IEEE Radar Conference (RadarConf20), Florence, Italy, 21–25 September 2020; IEEE: Piscataway Township, NJ, USA, 2020; pp. 1–6.
17. Schvartzman, D.; Curtis, C.D. Signal processing and radar characteristics (SPARC) simulator: A flexible dual-polarization weather-radar signal simulation framework based on preexisting radar-variable data. *IEEE J. Sel. Top. Appl. Earth Obs. Remote Sens.* **2018**, *12*, 135–150. [CrossRef]
18. Hernangómez, R.; Visentin, T.; Servadei, L.; Khodabakhshandeh, H.; Stańczak, S. Improving Radar Human Activity Classification Using Synthetic Data with Image Transformation. *Sensors* **2022**, *22*, 1519. [CrossRef]
19. Rahman, H. *Fundamental Principles of Radar*; CRC Press: Boca Raton, FL, USA, 2019.
20. Lara, F.; Ortiz, M.; Carrera, E.V.; Tinoco, A.F.; Moya, H.; León, R. Bayesian Processors of Radar Signals for the Skyguard Radar System of the Ecuadorian Army. *IEEE Lat. Am. Trans.* **2021**, *20*, 153–161. [CrossRef]
21. Mansouri, H.; Hamadouche, M.; Ettoumi, F.Y.; Magaz, B. Performance analysis of a Weighted Max CFAR processor. In Proceedings of the 2008 International Radar Symposium, Wroclaw, Poland, 21–23 May 2008; IEEE: Piscataway Township, NJ, USA, 2008; pp. 1–4.
22. Wang, S.; He, P. Research on Low Intercepting Radar Waveform Based on LFM and Barker Code Composite Modulation. In Proceedings of the 2018 International Conference on Sensor Networks and Signal Processing (SNSP), Xi'an, China, 28–31 October 2018; pp. 297–301. [CrossRef]
23. Pike, J. AN/TPS-70. Federation of American Scintists, Military Analysis Network. 1999. Available online: https://man.fas.org/dod-101/sys/ac/equip/an-tps-70.htm (accessed on 1 September 2023).
24. Lara, F.; Ortiz, M.; Carrera, E.V.; Tinoco, A.; León, R. Filtros adaptativos en el procesador bayesiano mti (moving target indicator) para el sistema de radar skyguard del ejército ecuatoriano. *Revista Ibérica de Sistemas e Tecnologias de Informaçao* **2020**, *E29*, 650–664. (In Spanish)
25. Turyn, R. Four-phase Barker codes. *IEEE Trans. Inf. Theory* **1974**, *20*, 366–371. [CrossRef]

Disclaimer/Publisher's Note: The statements, opinions and data contained in all publications are solely those of the individual author(s) and contributor(s) and not of MDPI and/or the editor(s). MDPI and/or the editor(s) disclaim responsibility for any injury to people or property resulting from any ideas, methods, instructions or products referred to in the content.